Supporting Information

Skillfully collaborating chemosynthesis with GOx-enabled tumor survival microenvironment deteriorating strategy for amplified chemotherapy and enhanced tumor ablation

Runxin Lu, Lin Zhou, Qijun Liu, Siqi Wang, Chunyan Yang, Li Hai, Li Guo* and Yong Wu*

Key Laboratory of Drug-Targeting and Drug Delivery System of the Education Ministry, Sichuan Engineering Laboratory for Plant-Sourced Drug and Sichuan Research Center for Drug Precision Industrial Technology, West China School of Pharmacy, Sichuan University, Chengdu 610041, P. R. China.

*Corresponding authors: guoli@scu.edu.cn (L. Guo), wyong@scu.edu.cn (Y. Wu).

Table S1. Characterization of different PTX-nanocarriers and GOx-nanocarriers. (data represent mean data ± SD, n=3).

Nanocarriers	Size(nm)	PDI	EE (%)	Zeta potential (mV)
PTX-NC	123.9±1.2	0.176±0.027	86.65±1.59	-1.36±0.48
PTX-RNC	118.8±2.6	0.217±0.038	90.77±1.11	9.51±0.39
PTX-BNC	139.5±1.7	0.122±0.015	95.60±2.18	-14.12±0.36
PTX-BRNC	147.9±1.3	0.171±0.019	94.92±1.27	-9.67±0.23
GOx-BRNC	161.4±1.9	0.176±0.015	12.27±1.35	-13.04±0.21

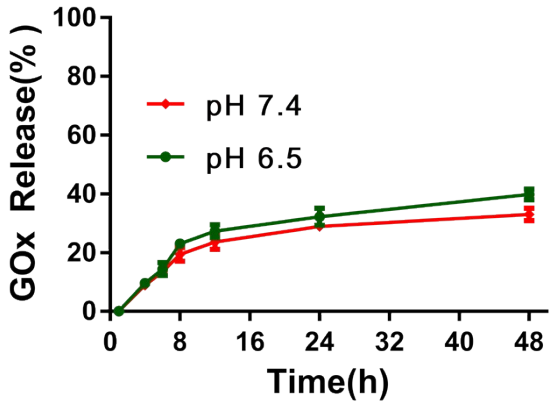

Figure S1. Cumulative GOx release of GOx-BRNC in PBS (pH 7.4 and 6.5) at 37 °C (Means ± SD, n = 3).

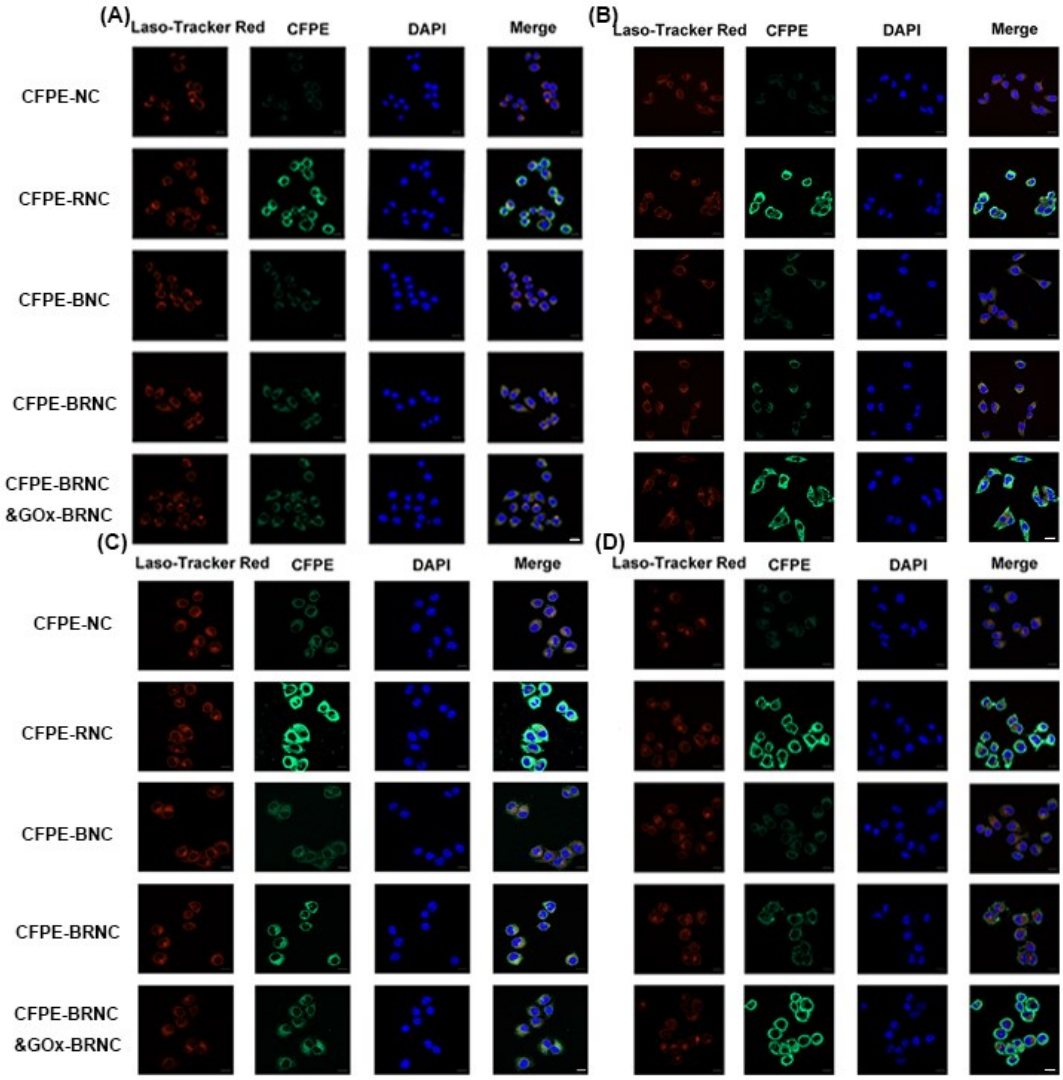

Figure S2. Colocalization of cells after incubation with different nanocarriers for 2h at pH 7.4 and pH 6.5. Confocal laser scanning microscopy (CLSM) images on 4T1 cells at pH 7.4 (A) and pH 6.5 (B), MCF7 cells at pH 7.4 (C) and pH 6.5 (D), showing FITC channel (green), LysoTracker-stained lysosome channel (red), and DAPI-stained nucleus channel (blue), the scale bar represents 20 μm.

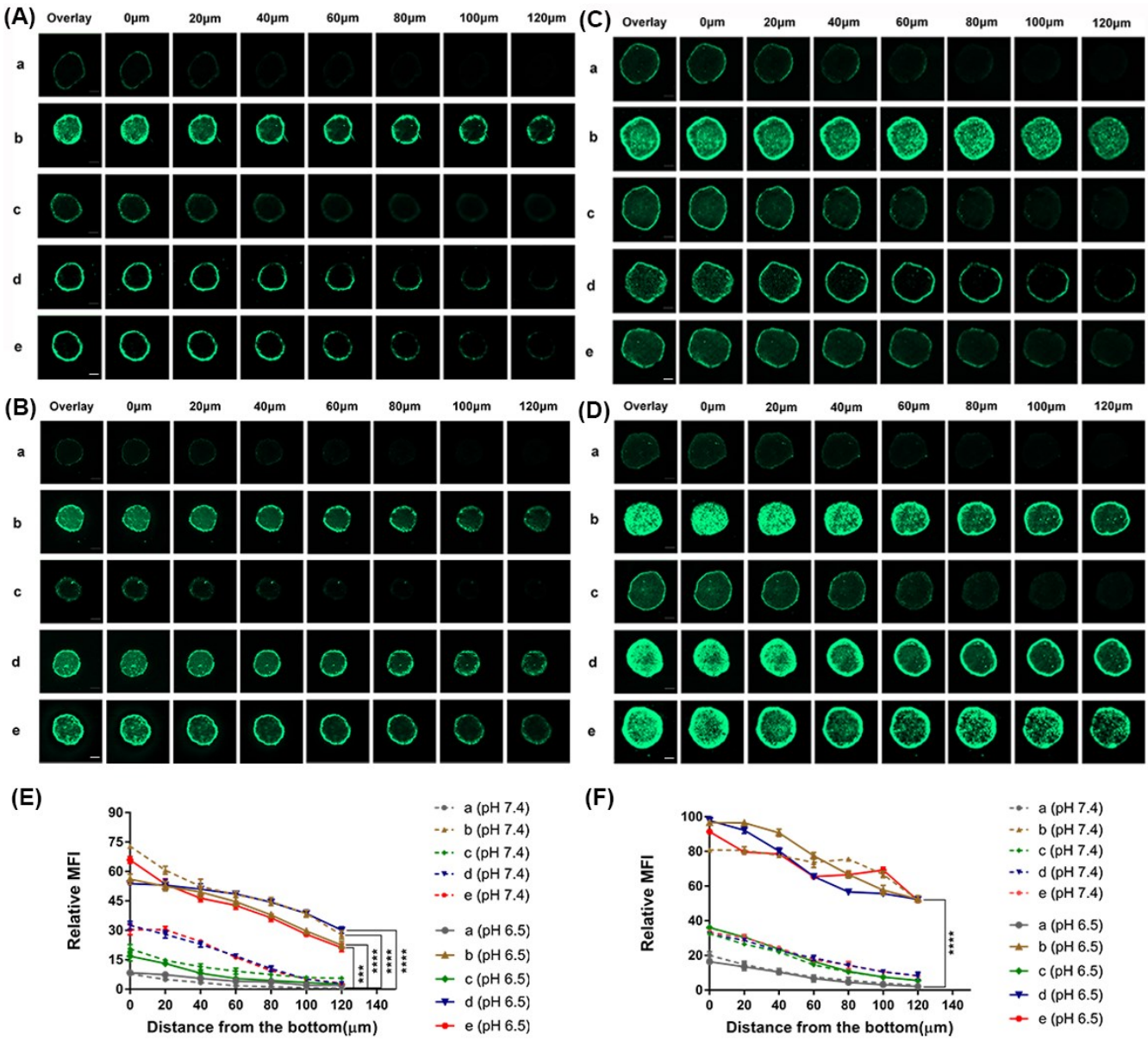

Figure S3. Tumor spheroids penetration. (A) and (C) were the fluorescence distribution of 4T1 and MCF7 tumor spheroids under pH=7.4 conditions, respectively. (B) and (D) were the fluorescence distribution of 4T1 and MCF7 tumor spheroids under pH 6.5 conditions, respectively. The concentration of CFPE was 2 μg/mL. (E) and (F) were the semi-quantitative intensity of these nanocarriers of 4T1 and MCF7 tumor spheroids, bars represent 100 μm ((a) CFPE-NC, (b) CFPE-RNC, (c) CFPE-BNC, (d) CFPE-BRNC, (e) CFPE-BRNC&GOx-BRNC) (Means ± SD, n = 3, **** indicates $p < 0.0001$ versus NC).

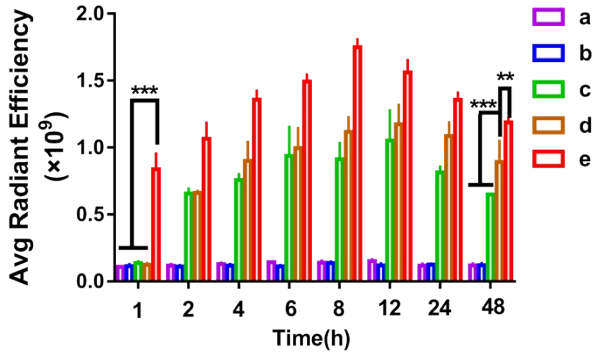

Figure S4. The semi-quantitative radiant efficiency of tumor measured by imaging ((a) DiD-NC, (b) DiD-RNC, (c) DiD-BNC, (d) DiD-BRNC, (e) DiD-BRNC&GOx-BRNC) (Means ± SD, n = 3, ** indicates $p < 0.01$, *** indicates $p < 0.001$).

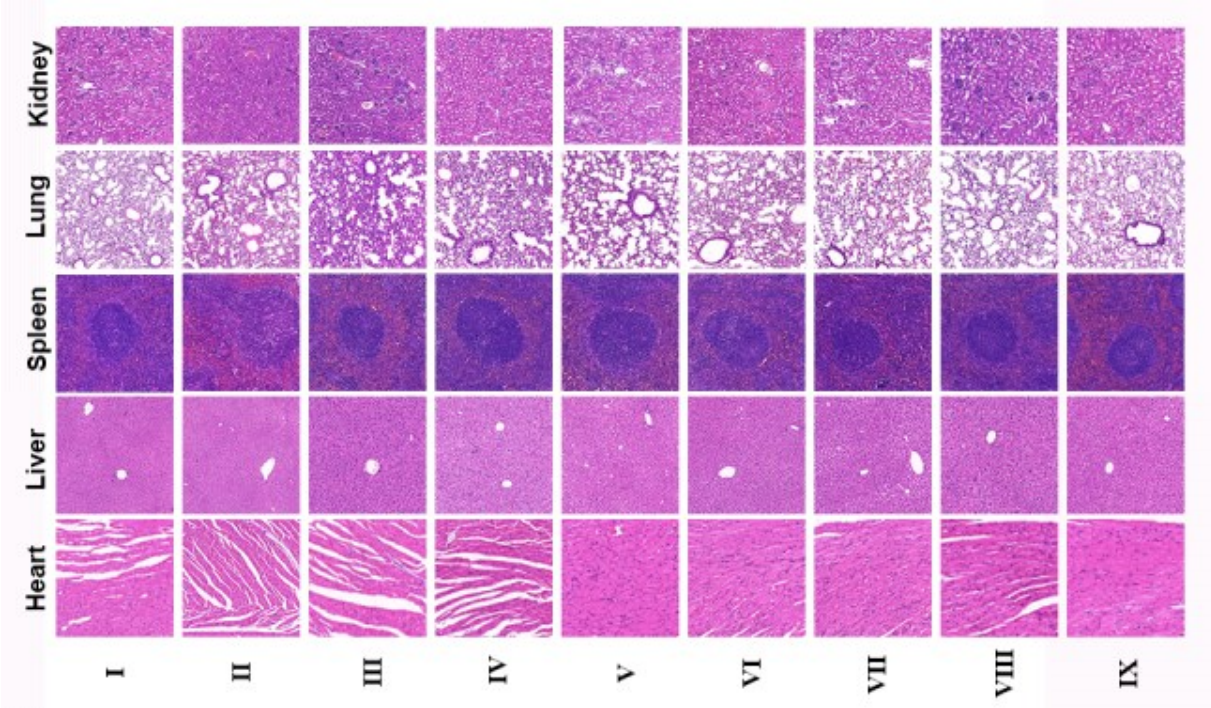

Figure S5. H&E analyses of the major organs (heart, liver, spleen, lung and kidney) after treatments of PBS (I), PTX (II), PTX-NC (III), PTX-RNC (IV), PTX-BNC (V), PTX-BRNC (VI), GOx-BRNC (VII), PTX-BRNC&GOx-BRNC (VIII, PTX=1 mg kg^{-1}), PTX-BRNC&GOx-BRNC (IX, PTX=3 mg kg^{-1}), and the scale bar represents 100 μm.

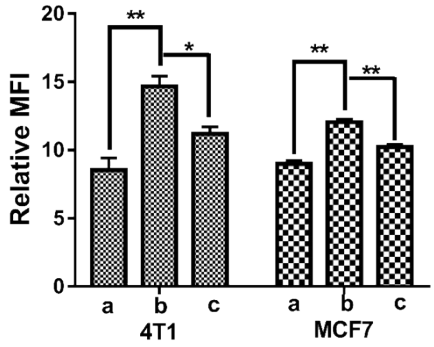

Figure S6. Biotin competitive inhibition experiment. The relative uptake of CFPE-BNC on 4T1 cells and MCF-7 cells for 2 h after pre-incubation with unlabeled biotin (1.5 mM) determined by flow cytometer ((a) CFPE-NC, (b) CFPE-BNC, (c) unlabeled biotin+CFPE-BNC) (Means ± SD, n= 3, *, ** represent $p < 0.05$, $p < 0.01$ versus CFPE-BNC group).

Figure S7. ^{1}H-NMR of compound **2**

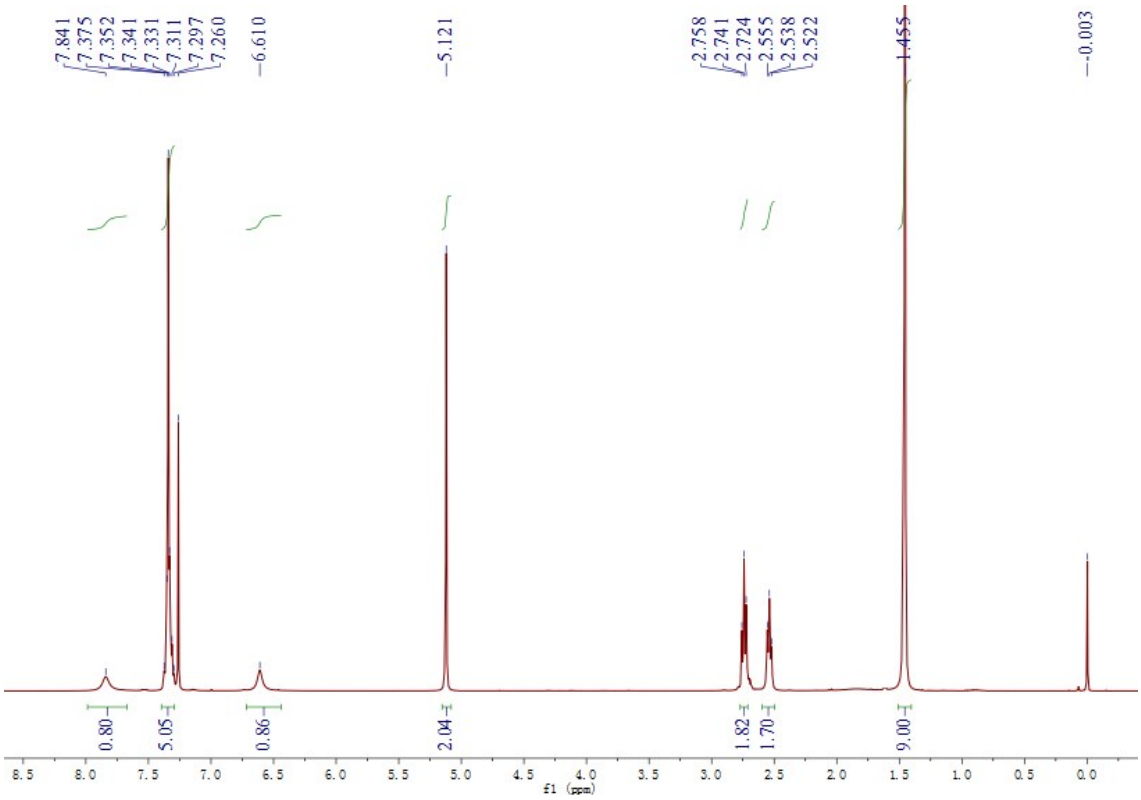

Figure S8. ^{13}C-NMR of compound **2**

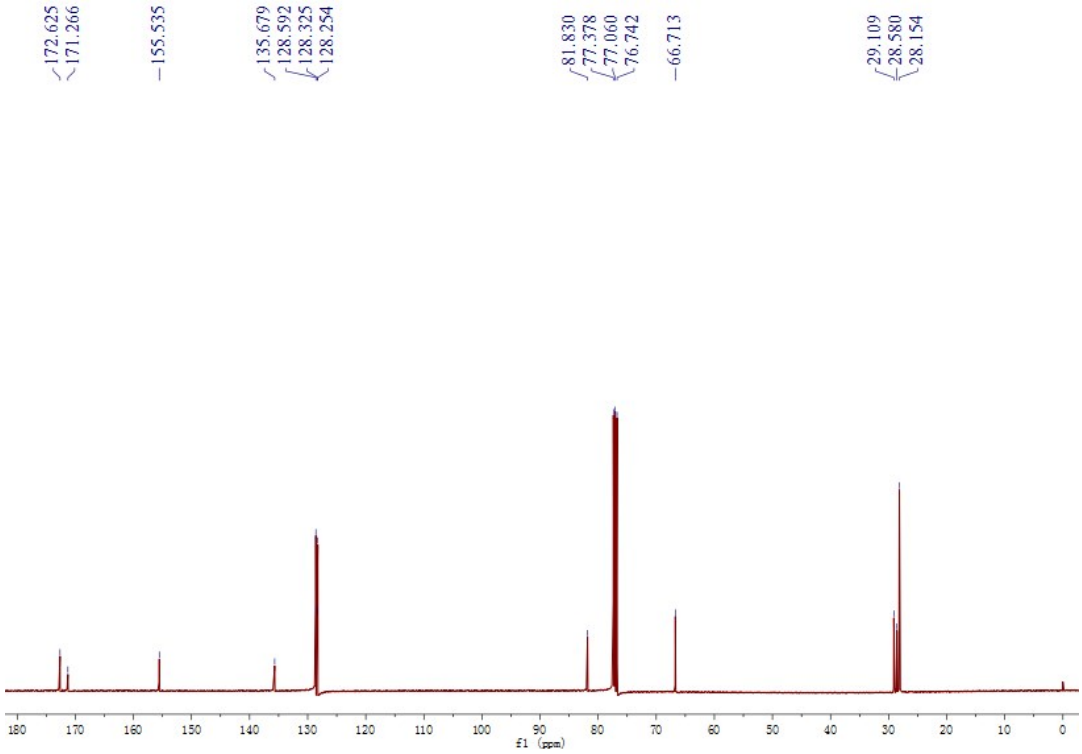

Figure S9. ^{1}H-NMR of compound **3**

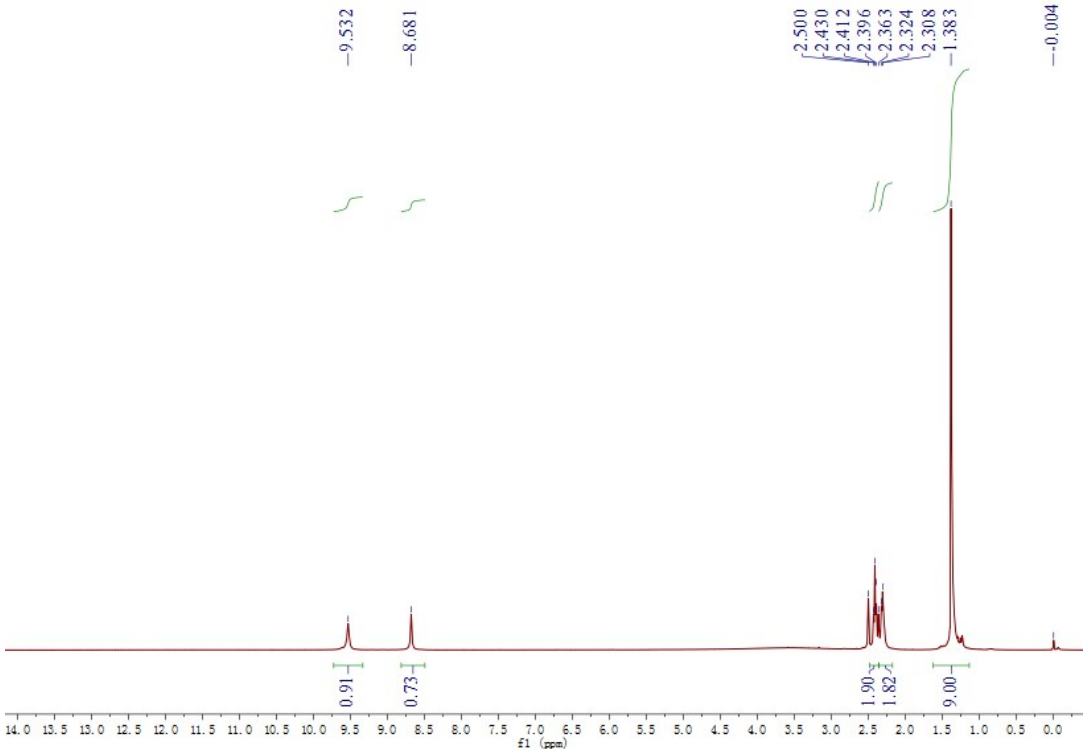

Figure S10. ^{13}C-NMR of compound **3**

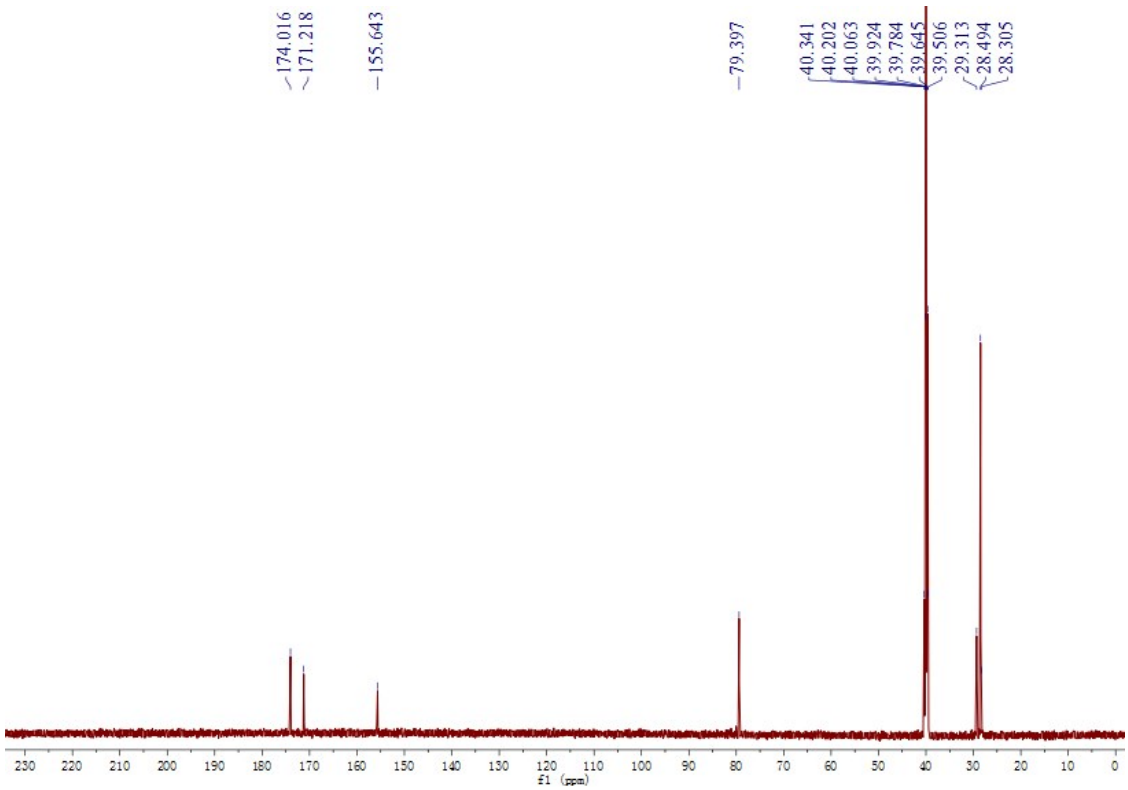

Figure S11. ^{1}H-NMR of compound **7**

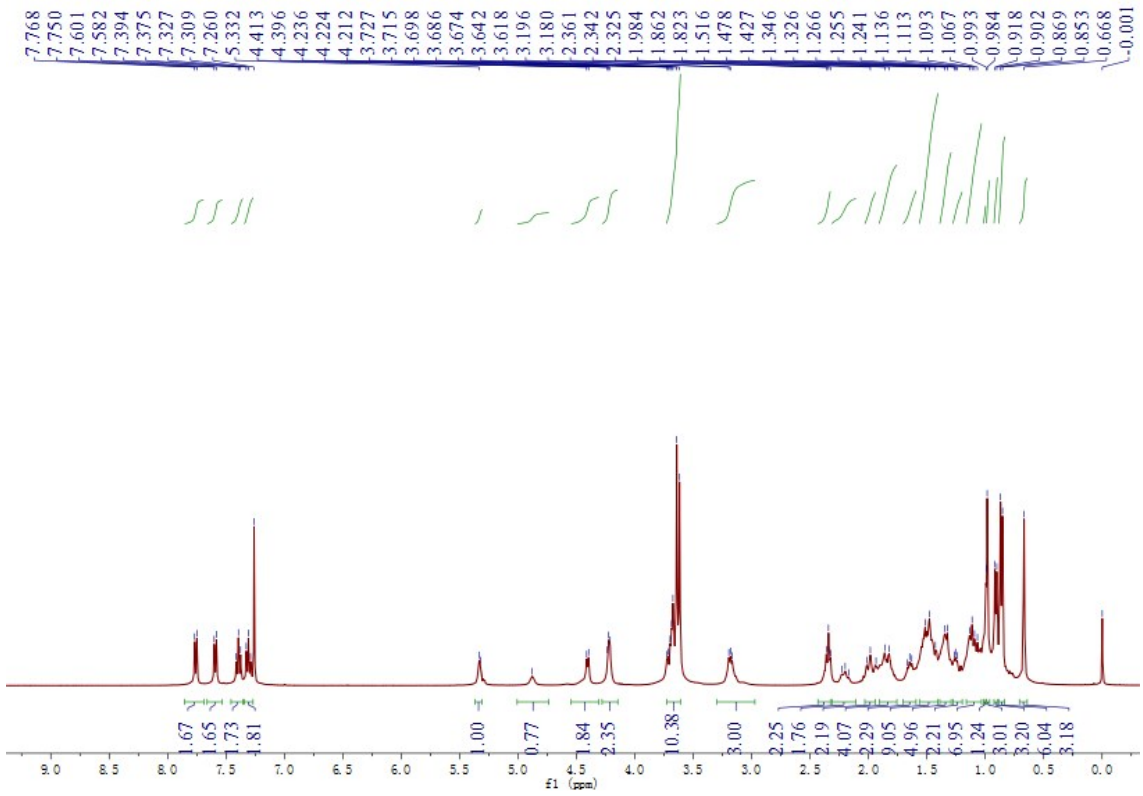

Figure S12. ^{13}C-NMR of compound **7**

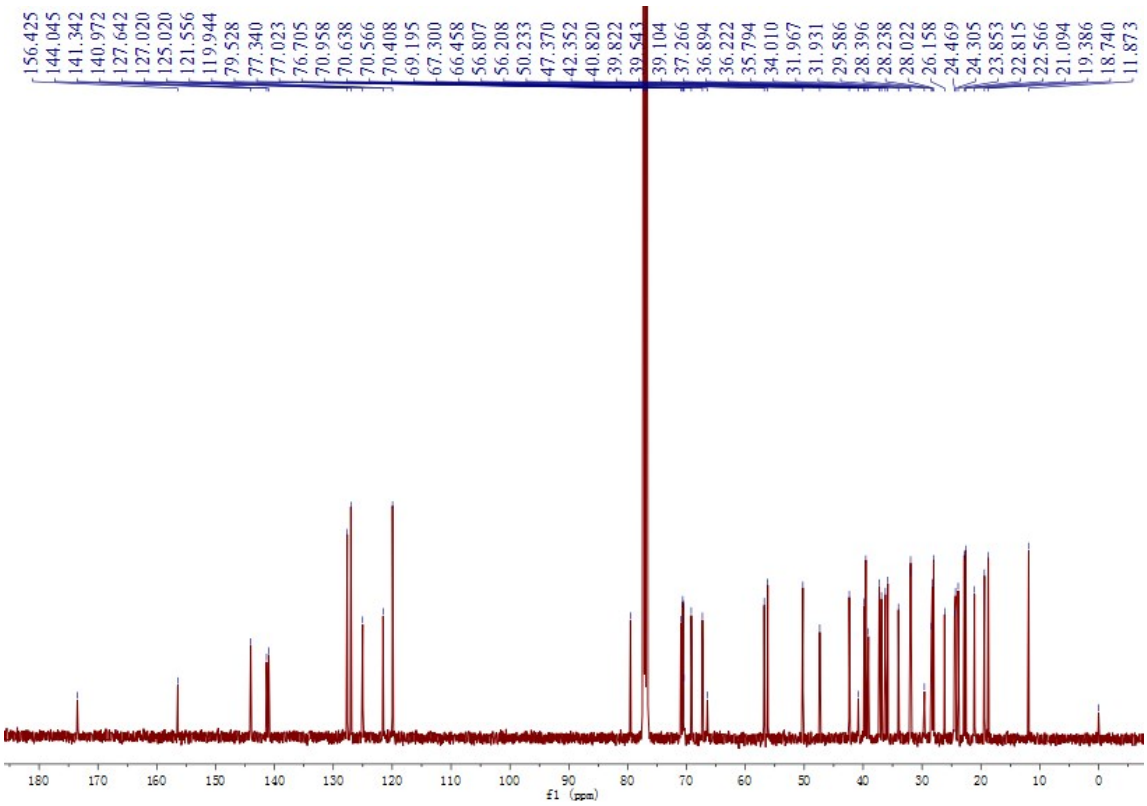

Figure S13. HR-MS of compound **7**

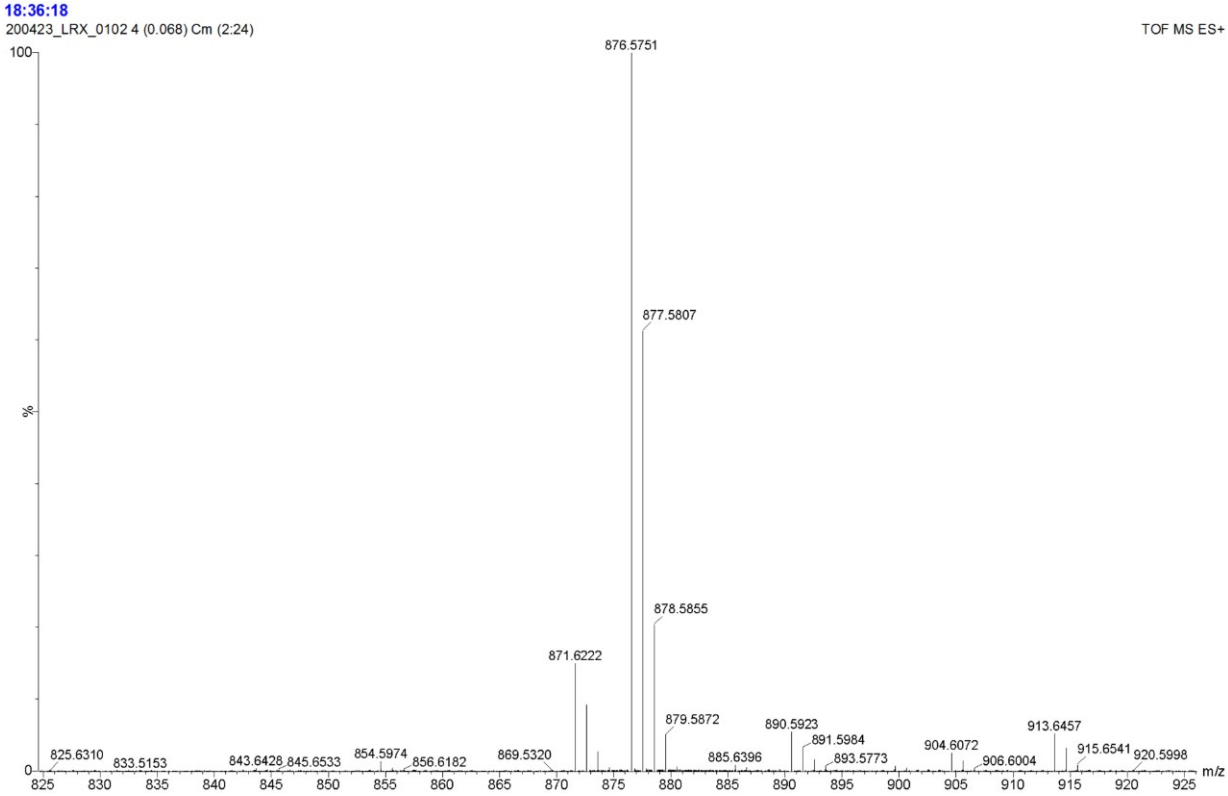

Figure S14. ^{1}H-NMR of compound **8**

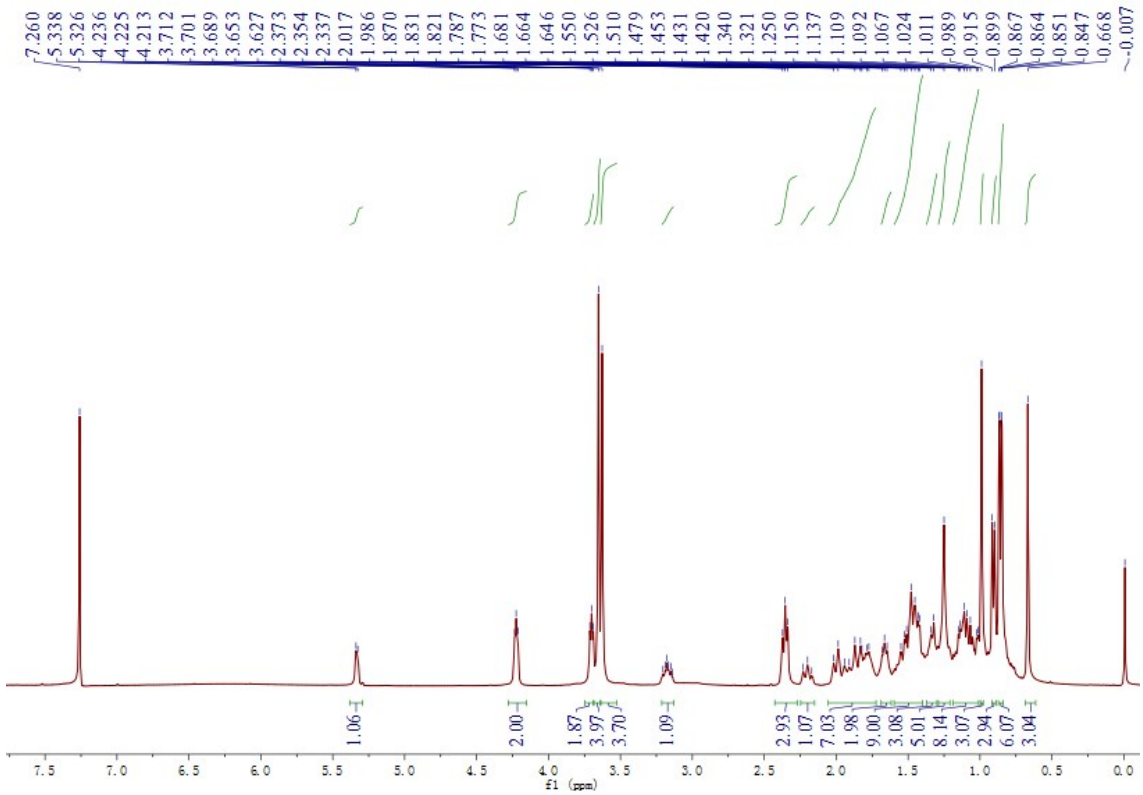

Figure S15. HR-MS of compound **8**

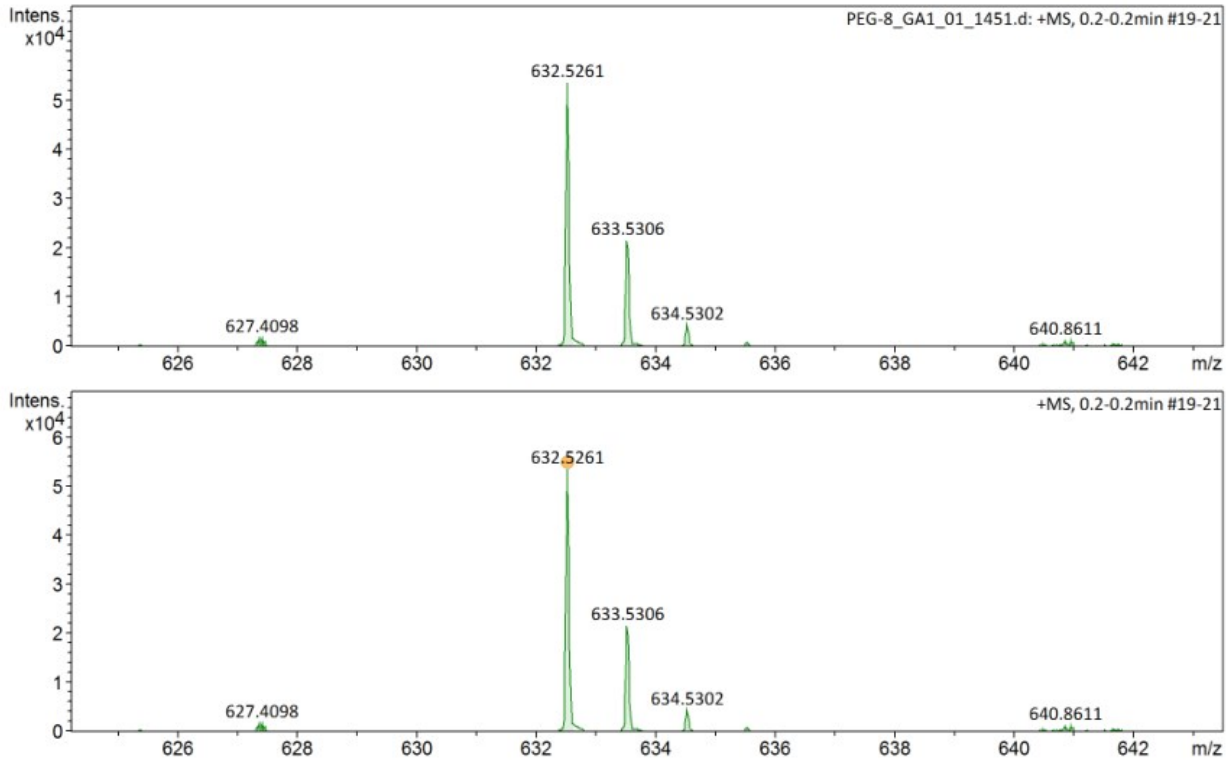

Figure S16. ^{1}H-NMR of compound **9**

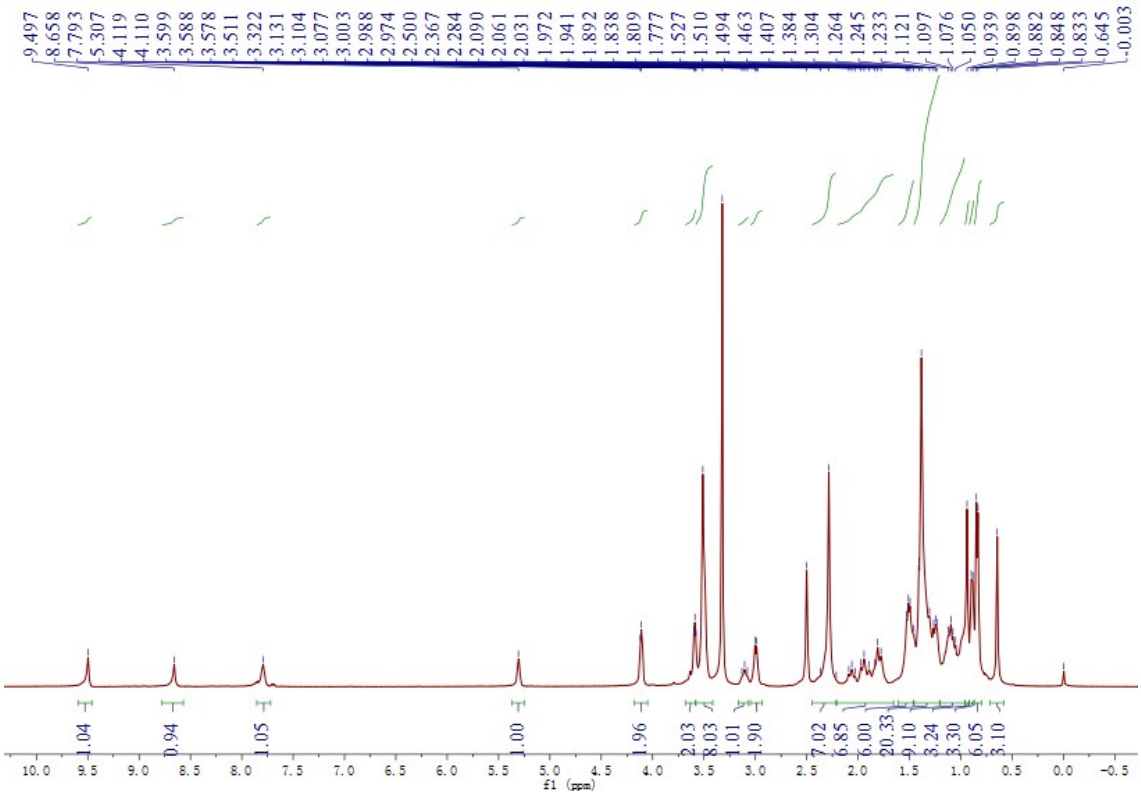

Figure S17. HR-MS of compound **9**

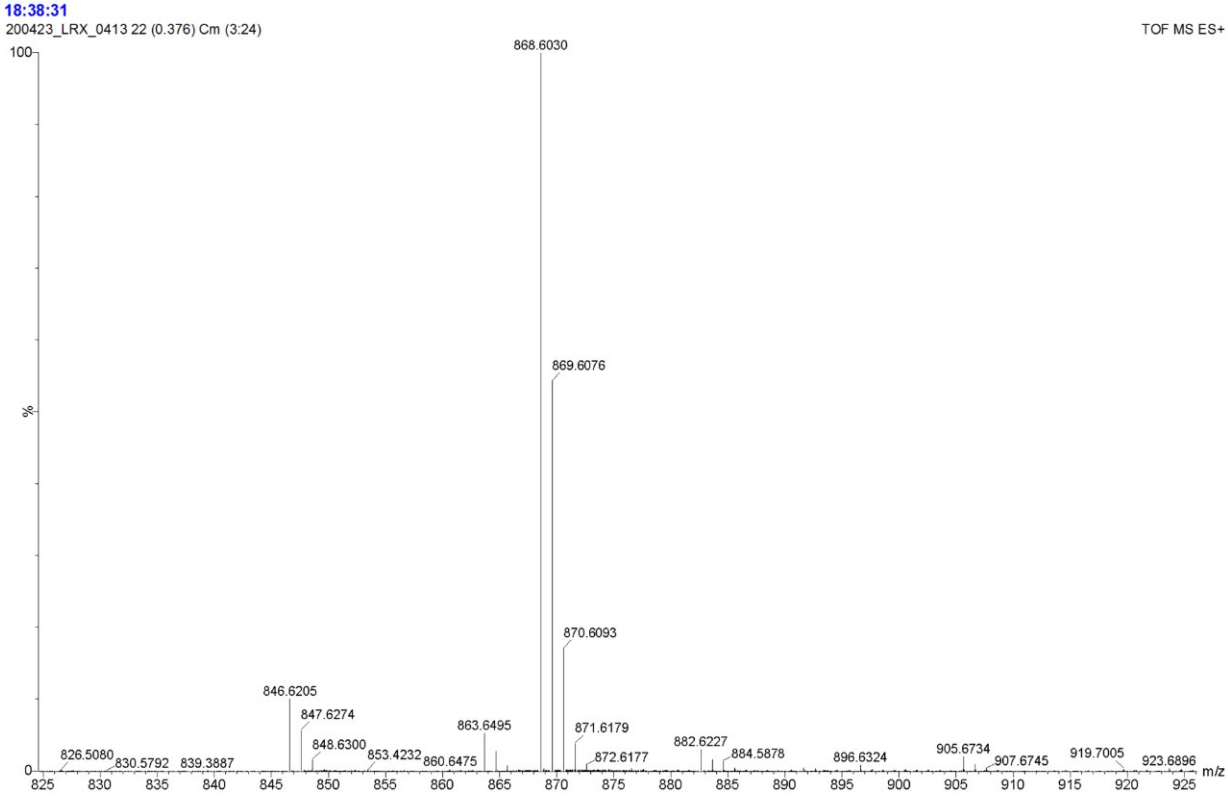

Figure S18. ^{1}H-NMR of compound **10**

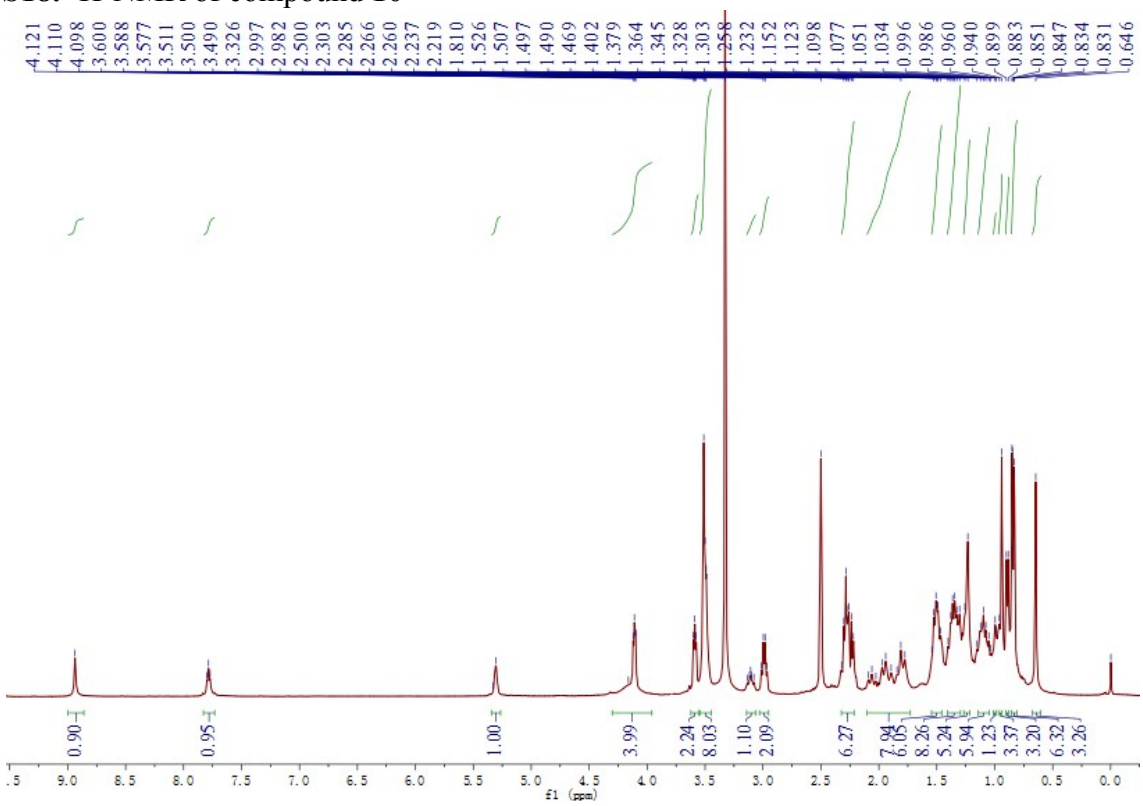

Figure S19. HR-MS of compound **10**

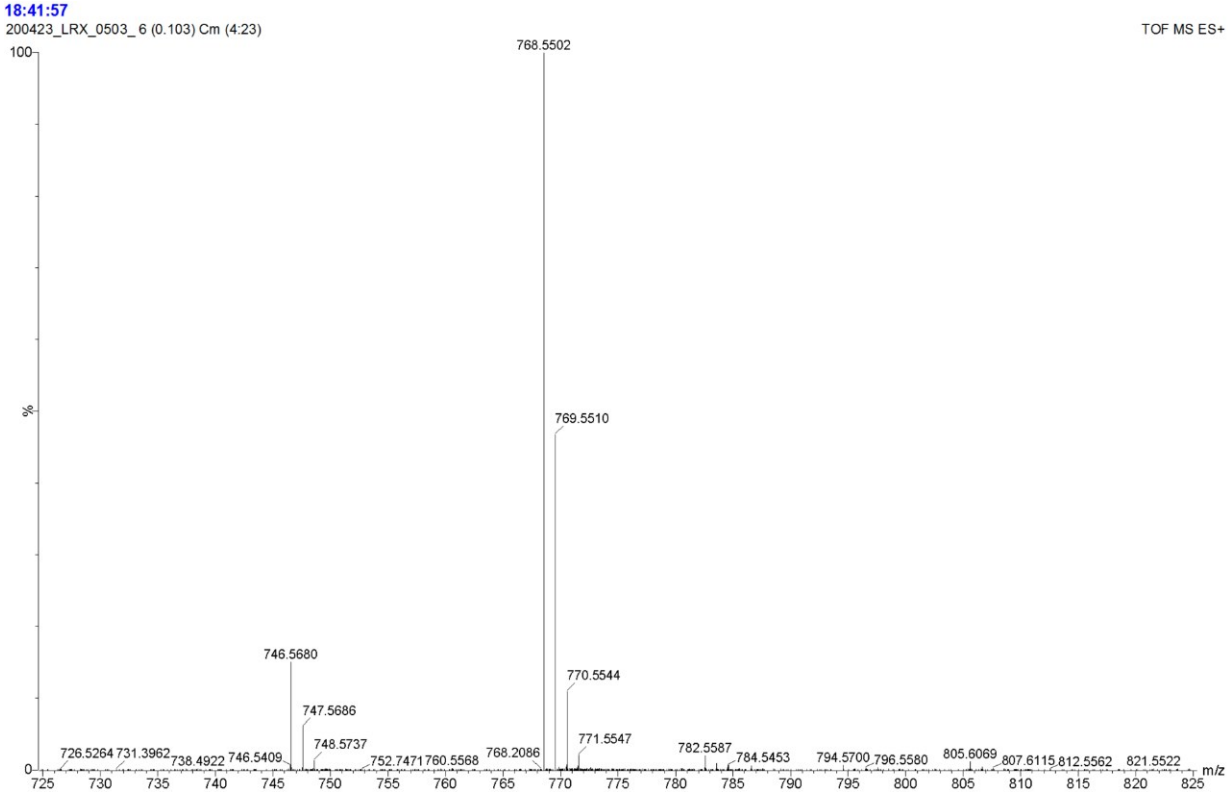

Figure S20. ^{1}H-NMR of compound **12**

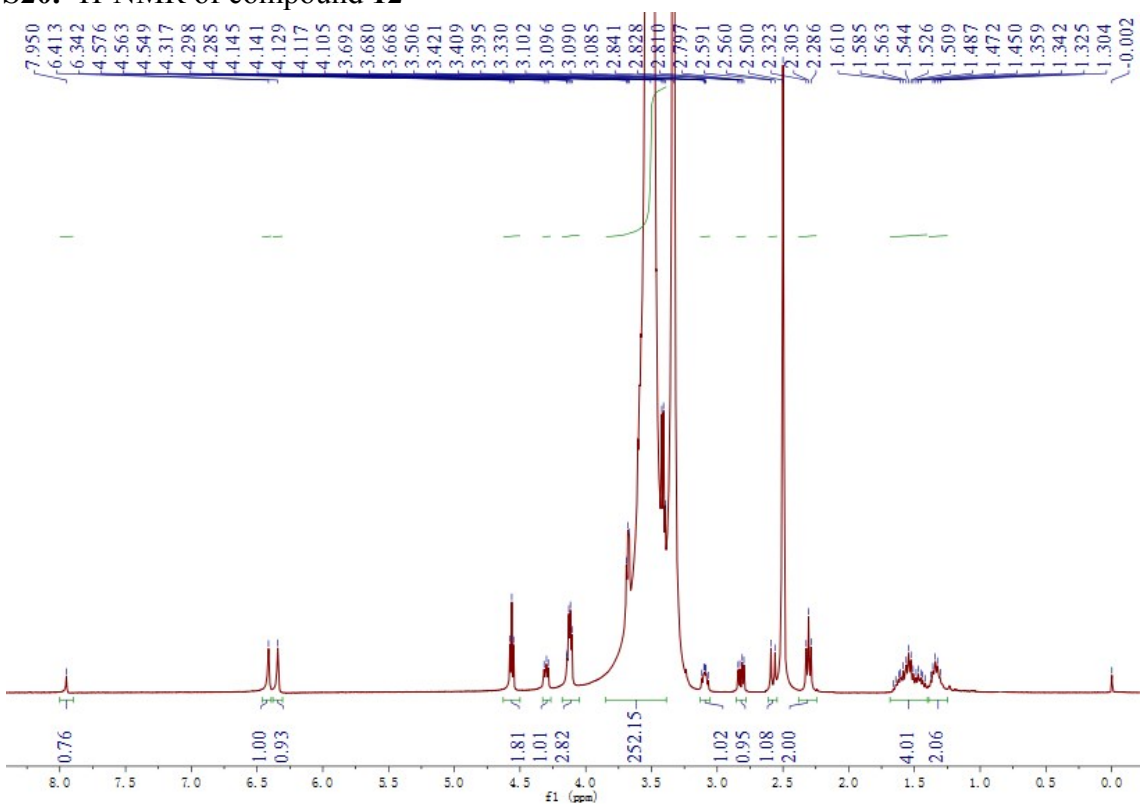

Figure S21. HR-MS of compound **12**

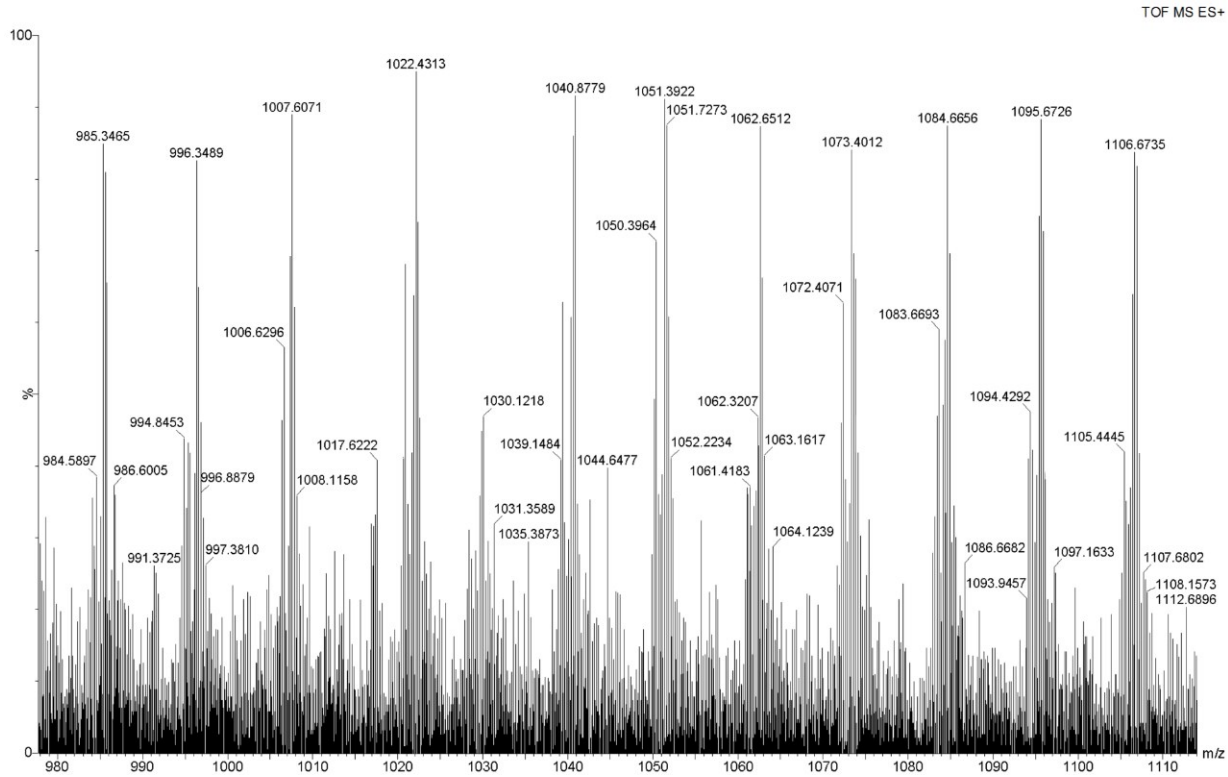

Figure S22. ^{1}H-NMR of compound **13**

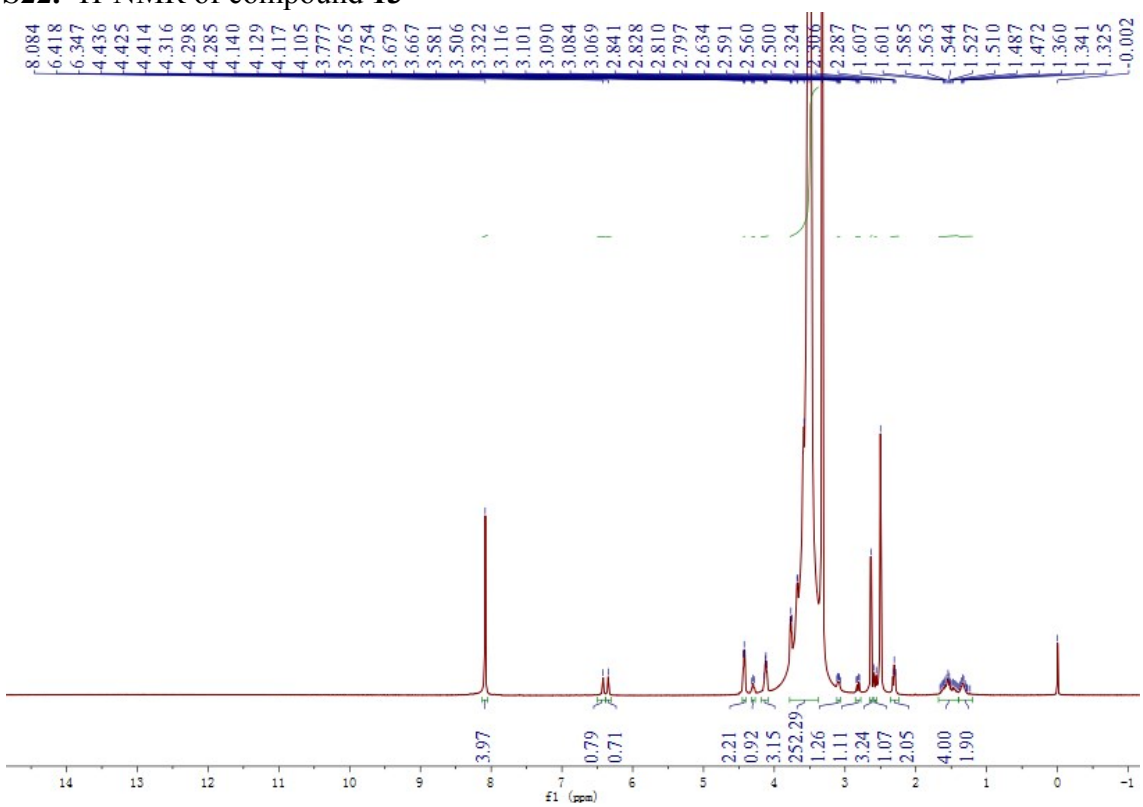

Figure S23. HR-MS of compound **13**

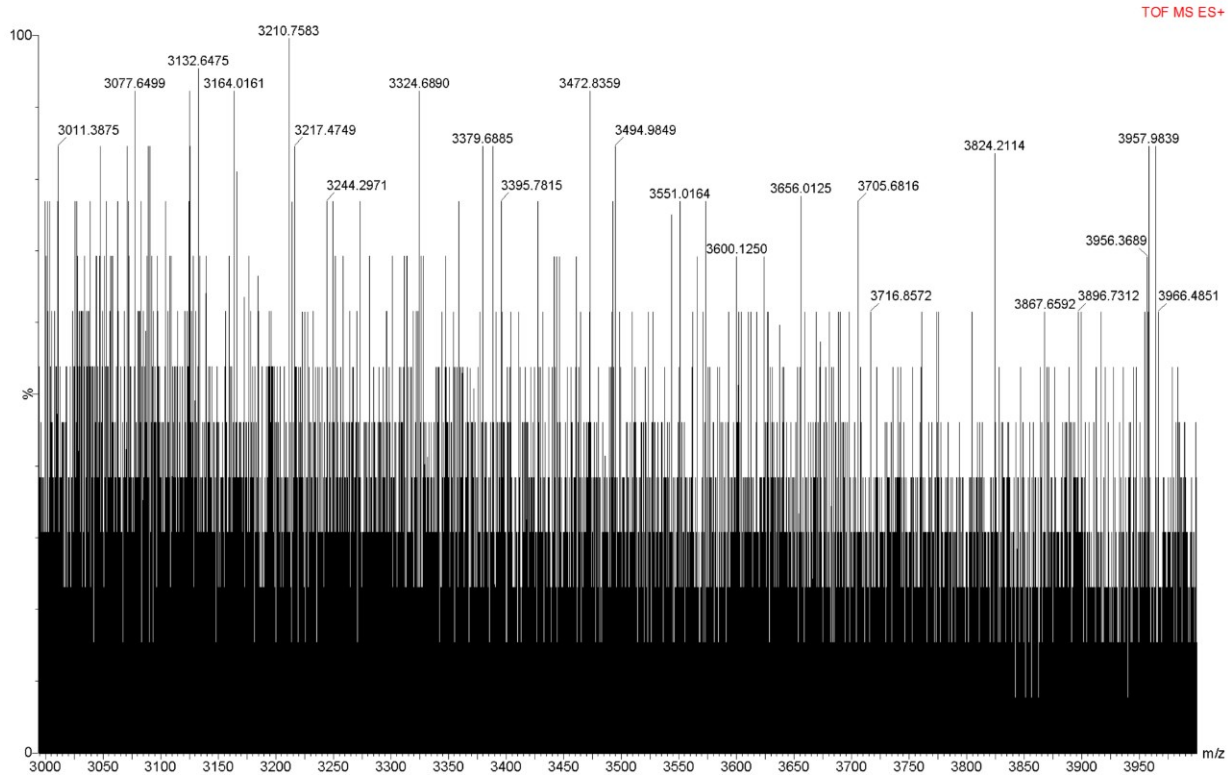

Figure S24. ^{1}H-NMR of ligand **Bio-PEG$_{3350}$-Hz-Chol**

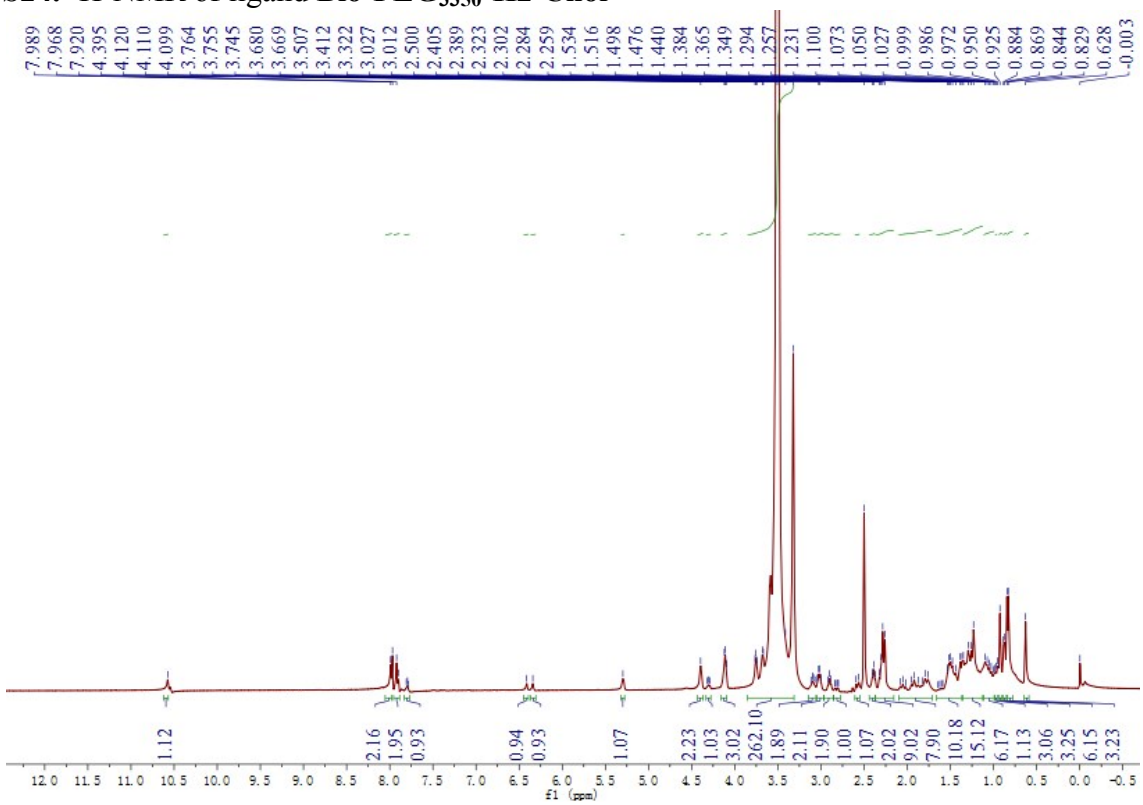

Figure S25. HR-MS of compound **Bio-PEG$_{3350}$-Hz-Chol**

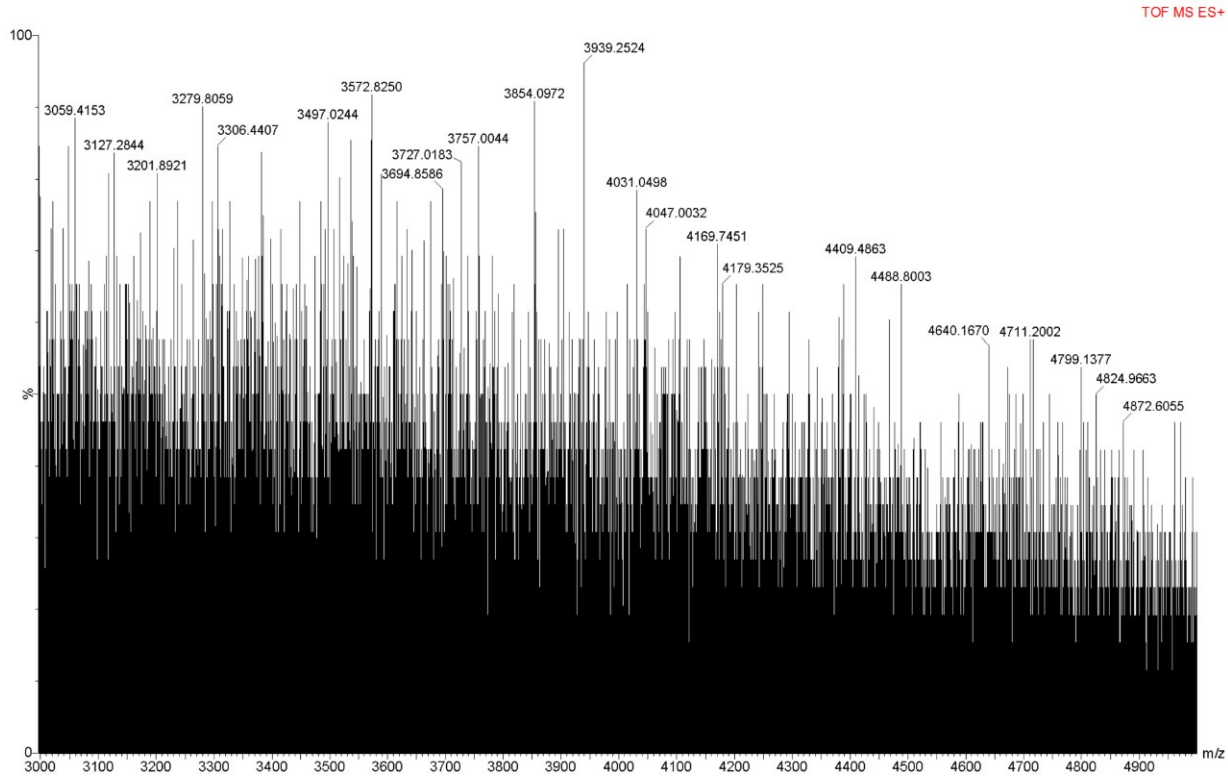

Figure S26. ^{1}H-NMR of ligand **DSPE-PEG$_{2000}$-R$_8$**

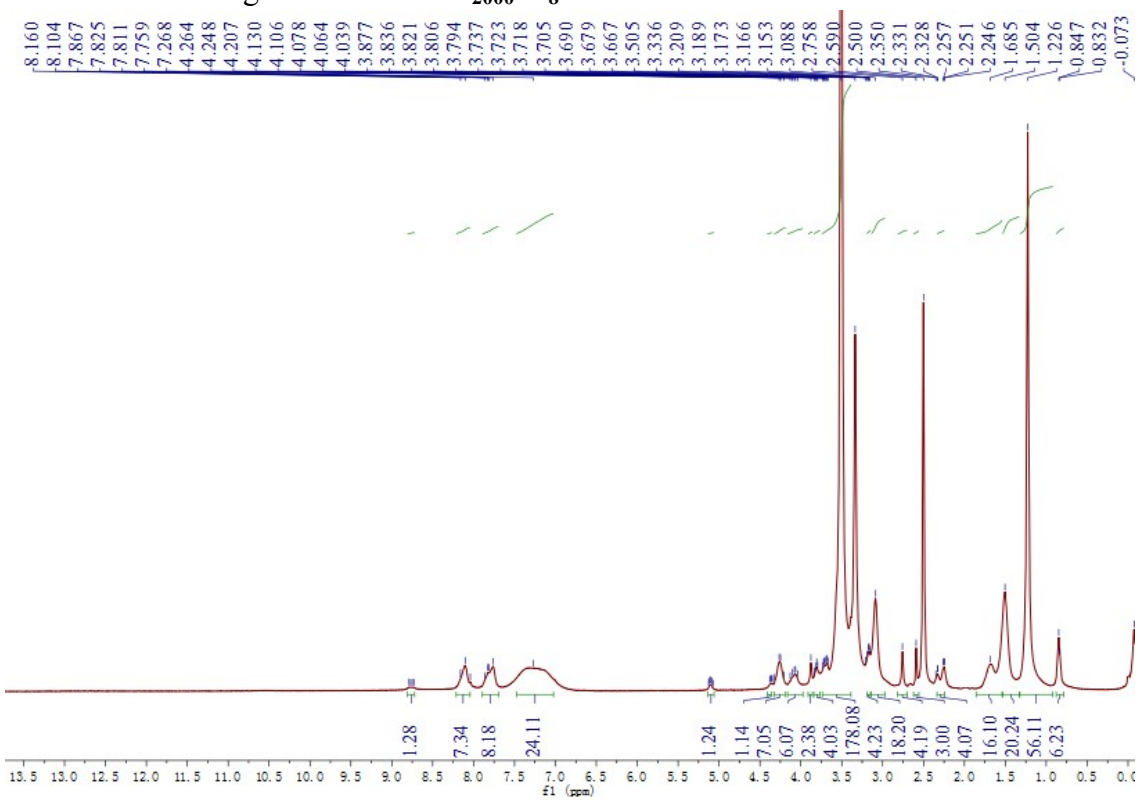

Figure S27. HR-MS of compound **DSPE-PEG$_{2000}$-R$_8$**